Original Article
Full-thickness wound healing using 3D bioprinted gelatin-alginate scaffolds in mice: a histopathological study

Jing Liu[1*], Jinghua Chi[1*], Kaixi Wang[2], Xiaoping Liu[1], Jie Liu[3], Fang Gu[1]

[1]Qingdao University Medical College, Qingdao, Shandong, China; [2]Department of Orthopedic Surgery Musculo-skeletal Research Center Washington University in Saint Louis Tang Lab, USA; [3]The Affiliated Hospital of Qingdao University, Qingdao, Shandong, China. *Equal contributors.

Abstract: This study aimed to determine the effect of the 3D bioprinted gelatin-alginate scaffold on the full-thickness skin wound healing on mouse back and to observe the histopathological changes during the wound healing process. Using a murine wound model, full skin thickness excisions were created on the dorsum of 40 mice. Then, each mouse was randomly assigned to either the control group or treatment group, in which the surface of the wound was either covered with a traditionally used ointment or the bioactive scaffold, respectively. The bioactive scaffold consisted of a layered gelatin-alginate polymer grid containing regular holes of an appropriate size that was printed using a 3D bioprinter. Efficacy was determined by qualitative comparisons of photographs of the wounds during healing as well as histopathological changes of tissue samples taken throughout the healing process. It was observed that the average healing time of the control mice was 16±1 days, while that of the treatment mice was 14±1 days. Futher histological analysis also revealed improved healing in the treatment mice. Overall, our results suggest that the gelatin-alginate bioactive scaffold accelerates skin wound healing through facilitating granulation and scar tissue formation.

Keywords: 3D bioprinting, gelatin-alginate scaffold, histopathology analysis, wound healing

Introduction

The skin is the largest organ of the body and serves as the body's primary defense against the external environment. As the first physical barrier to any stress or trauma, the skin is particular prone to injury. While most superficial skin wounds heal naturally with time, limitations of skin biomechanics make it difficult for large area skin wounds caused by mechanical trauma, surgical procedures or burns to heal without additional interventions. Furthermore, the potential life-threatening fluid loss, hemorrhagic shock, and infection immediately following large skin lesions during the early stages of healing makes medical treatment imperative. Skin grafts have traditionally been used to treat large skin lesions. However, the use of full-thickness skin grafts is limited by size and source site, as the requirement to harvest skin from a donor site to graft onto the trauma site

puts the patient at risk of additional complications. Therefore, an increasing number of researchers have explored more favorable methods for large area wound repair [1-3]. Emerging techniques using 3D bioprinting, have shown great potential as an alternative [4]. Using a 3D bio-printer, this technique involves printing bioactive substances to prepare synthetic biocompatible scaffolds that replace traditional skin grafts. By similarly covering the wound, the scaffolds can decrease excessive bleeding exudate production and infection probability at the wound site [5, 6]. The biocompatible and porous structures of these scaffolds facilitate cell adhesion and migration, material exchange, and deep tissue growth in the wounds [7, 8]. Moreover, compared to other methods for preparing bioactive scaffolds [9-11], the use of 3D bioprinting allows for more flexibility and repeatability, as complete 3D structures can be designed according to pre-

determined size and porosities using CAD software and printed using an automated 3D printer. Whilst the use of scaffolds in skin tissue engineering has been well-studied, few studies refer to the systematic histopathological study during the wound healing, particularly the use of a 3D bioprinted gelatin-alginate scaffold on full-thickness skin wound murine wound models.

Therefore, this study used an *in vivo* full-thickness skin wound murine model to compare the healing of wounds treated with a gelatin-alginate hydrogel versus a traditional dressing. Additionally, the histopathological changes within both groups were compared to explore the function and potency of scaffolds during the wound healing process. Altogether, this study provides an efficient method to prepare scaffolds and furthers the research on scaffold use in animal models.

Materials and methods

Preparation of porous gelatin-alginate bioactive scaffolds

Stock solutions of gelatin (5 mg/ml) and alginate (25 mg/ml) were prepared by dissolving gelatin and an alginic acid sodium salt, respectively, in phosphate-buffered saline (PBS). After intermittent sterilization of the two stock solutions, a pre-polymer solution was made by thoroughly mixing the gelatin and alginate solutions in predetermined proportions. The pre-polymer solution was loaded into the cartridge of the 3D bioprinter, which had been programmed with parameters preset by a computer control system. Under aseptic conditions, the pre-polymer solution was extruded as strands through a 300 μm nozzle attached to the 3D printer and deposited layer-by-layer into a culture dish to form a 3D mesh pattern.

Once printing was complete, the patterned 3D structure was immersed in 100 mM $CaCl_2$ for 10 min to allow complete crosslinking of the polymers and form the functional 3D bioactive scaffolds patterned with a 300 μm grid.

Animal experiments

All the animal experiments were reviewed and approved by the Council of Science and Technology of Qingdao University.

Forty, 6-week-old female mice (scxkLu2013-0001, 25±5 g) were used in this study. Prior to experiments, the mice were housed individually in clean cages under controlled conditions (12 h light-dark cycle at 22-25°C and 60-70% relative humidity) for 2 weeks to allow time to acclimatize. On day 0, a full-thickness dorsal excision was surgically made on the dorsum of each mouse to model full-thickness wounds. For all operations, mice were anesthetized with an intraperitoneal injection of pentobarbital sodium. A 3×3 cm patch of fur on the dorsal side was removed with 8% Na_2S aqueous solution, as previously described [12] and the area was disinfected with 3% iodophor and 75% ethanol. Methylene blue was used to mark a 1 cm circular area on the exposed dorsal skin and a full-thickness excision was made using incision scissors [13]. After, the mice were randomly assigned to either the control (n=20) or the treatment (n=20) group. In the control group, the wounds were topically treated with vaseline and dressed with a thin gauze secured by an elastic bandage. In the treatment group, the wound was immediately covered with the bioactive gelatin-alginate scaffold after excision and dressed with thin gauze secured by an elastic bandage. The wounds of both groups were observed and imaged at various time points after wounding. For quantitative measurements, a dividing ruler was set at the same level as the wound sites, as a reference.

Histological study

Wound tissue samples and 0.5 cm of normal skin, from both groups, were harvested on day 1, 3, 7, and 14, respectively, after wound injury, for histological analysis. Samples were fixed in 4% paraformaldehyde solution (pH 7.4) for 24 h, dehydrated, cleared and embedded in paraffin. Sections (5 μm-thick) were mounted on adhesive glass slides and stained with hematoxylin-eosin (HE), using standard procedures. The stained tissue sections were observed and the images captured under a light microscope (Olympus BX3-CBH).

Statistical analysis

The average diameter of the wounds was compared between the treatment and control group by an unpaired Student's *t*-test using SPSS statistical software (IBM, the USA). A P<0.05 was considered significant.
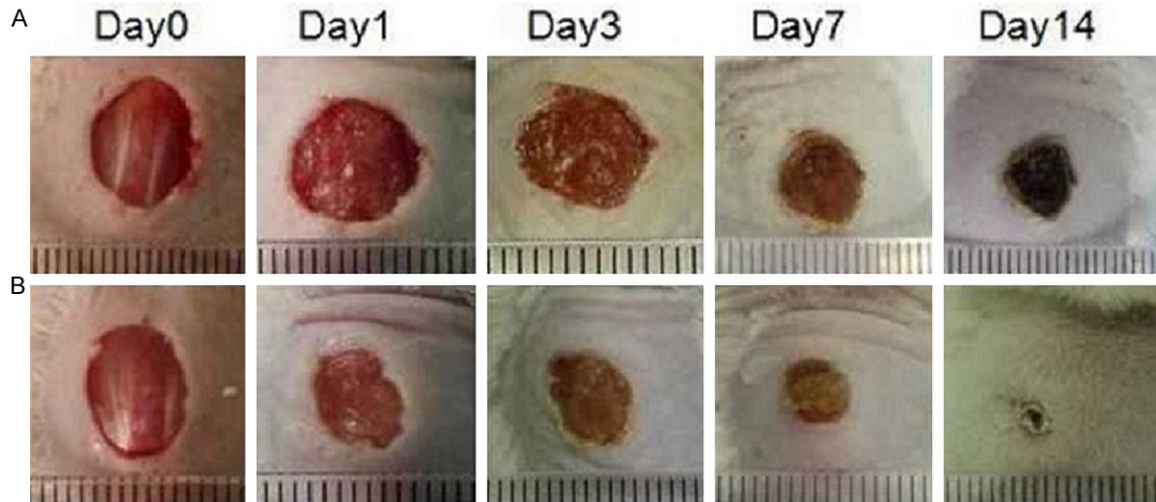
Figure 1. The changes in the wound surface of the control group (A) and experimental group (B) on day 0, 1, 3, 7, and day 14 after injury.

Results

Gross observations during wound healing in mice

Skin wound healing was evaluated by photographic images. **Figure 1** shows the wound size changes. A circular wound (1 cm diameter) was induced in the dorsal skin of each mouse using an incisive scissor, in both the control (**Figure 1A**) and treatment group (**Figure 1B**). Each defect was deep into the subcutaneous tissue, thus, obvious bleeding was observed during the wound excision. After, the area around the wound was swollen and slightly red. In the treatment mice, the scaffolds covering the wound realized the attachment to the wound tissue. Twenty-four hours later, swelling in the area around the wound was observed in the control group and the wound area had slightly decreased. The scaffolds of the treatment group combined with the edges of the wound, where swelling was evident. Consequently, the edges of the wounds were directed toward the center to form wounds with a 0.8 cm average diameter. On day 3 after injury, the surface of the wound in both the control and treatment groups became dry, swelling around the wound subsided and it gradually began to form a pale yellow crust; wound area had decreased in both groups but wounds in the control group were still circular with a 0.8-0.9 cm diameter, while those in the treatment group were irregularly oval or circular with a 0.7-0.8 cm diameter and a softer texture. On day 7 after injury, swelling in both groups disappeared and the edges had subsided. The wound crust color had visually deepened in the control group compared to the treatment group and had a harder texture. The wound mean diameter was 0.7 cm in the control group and 0.5 cm in the treatment group. Until day 14, the wound surface of the control mice was covered with pale black, hard crusts (0.7 cm mean diameter), part of them could be peeled and tender skin tissue was exposed beneath (**Figure 1A**). In the treatment group, the wound had almost completely healed with a thin or no crust. The mean diameter of the tougher scar was 0.2 cm (**Figure 1B**).

Histological study

On day 1, light microscopy showed breakage of skin and subcutaneous tissue was visible in both the control and treatment groups (**Figure 2**, ×40). There were obvious hemorrhage, tissue necrosis and a lot of exudates from the surface to a deep layer of the wound area (**Figure 2**, ×100). At high magnification, a large amount of serous and fibrinous exudates in both groups was observed and there were visible signs that the inflammatory response had occurred. Leukocyte infiltration was given priority to a large number of neutrophils and small amounts of macrophages (**Figure 2**, ×400).

On day 3, the wound surface of both groups was covered with a crust, but the crusts of the control group were thicker than those of the
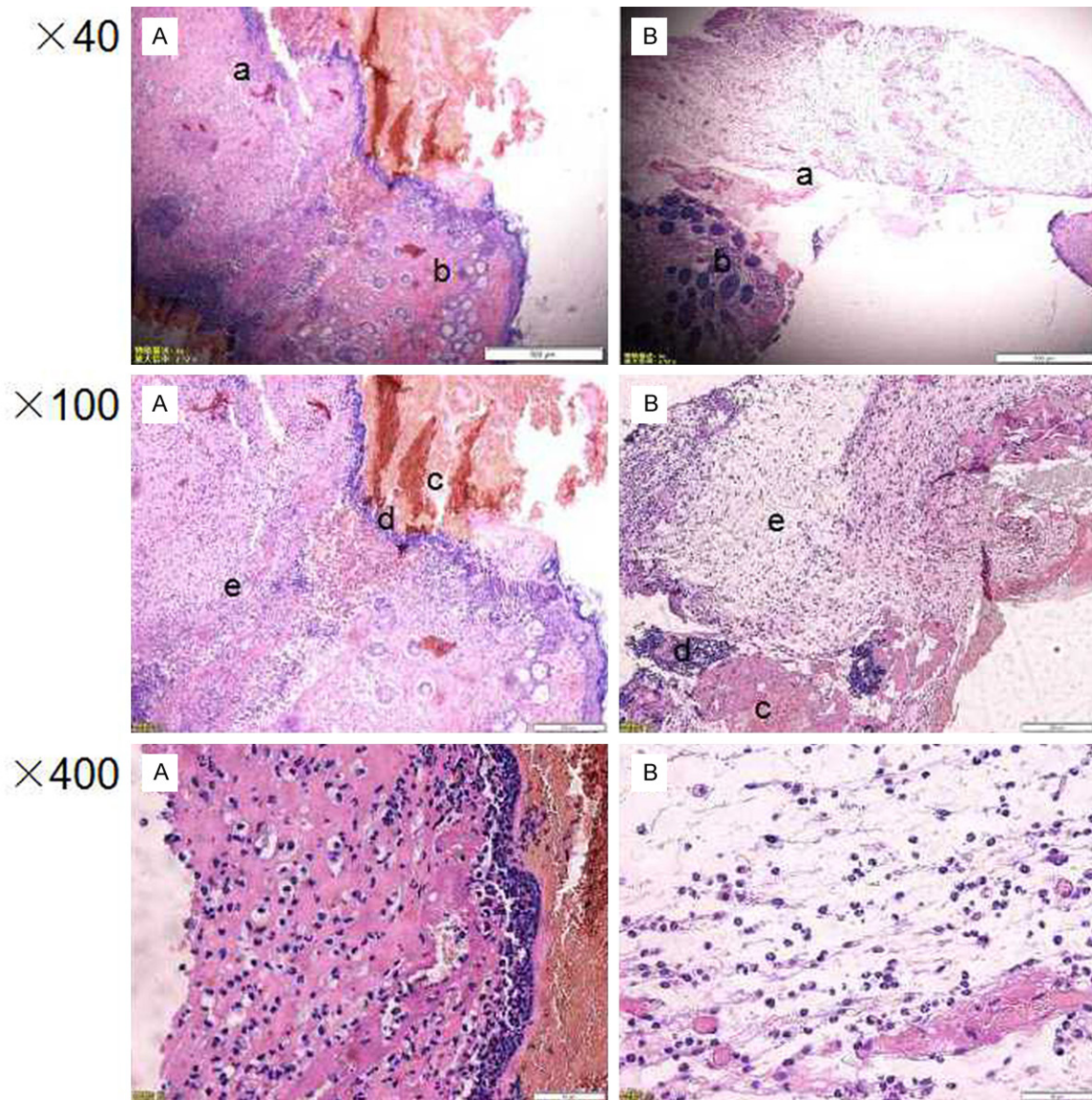
Figure 2. Representative micrographs of wound healing on day 1 (HE staining) in the control group (A) and treatment group (B) under ×40, ×100, and ×400 magnifications. Tissue defect (a), remaining skin tissue (b), hemorrhage (c), tissue necrosis (d), and exudates (e).

treatment group. The whole layer of skin and subcutaneous tissue at the edges of the wound had moved to the center of the wound (**Figure 3**, ×40). Also, a large amount of fresh granulation tissue appeared at the edges and the base of the wound in both groups. However, there was less necrosis and exudate residual on the surface of the granulation tissue in the treatment group than the control group (**Figure 3**, ×100). As shown in **Figure 3**, the crusts consisted of necrotic tissue, fibrin, blood and others. The neutrophils in the exudates had disintegrated. The scaffold between the crust and

necrotic tissue was visible in the treatment group, while the scaffold between the necrotic layer and granulation tissue had dissolved (**Figure 3**, ×200).

On day 7, fresh epidermal tissue grew beneath the crusts in both the control and treatment groups. However, the crusts in the treatment group had thickened, while the crusts in the control group had decreased (**Figure 4**, ×40). In the center of the wound in both groups, large amounts of exudates and necrosis remained but had disappeared from the wound edges of
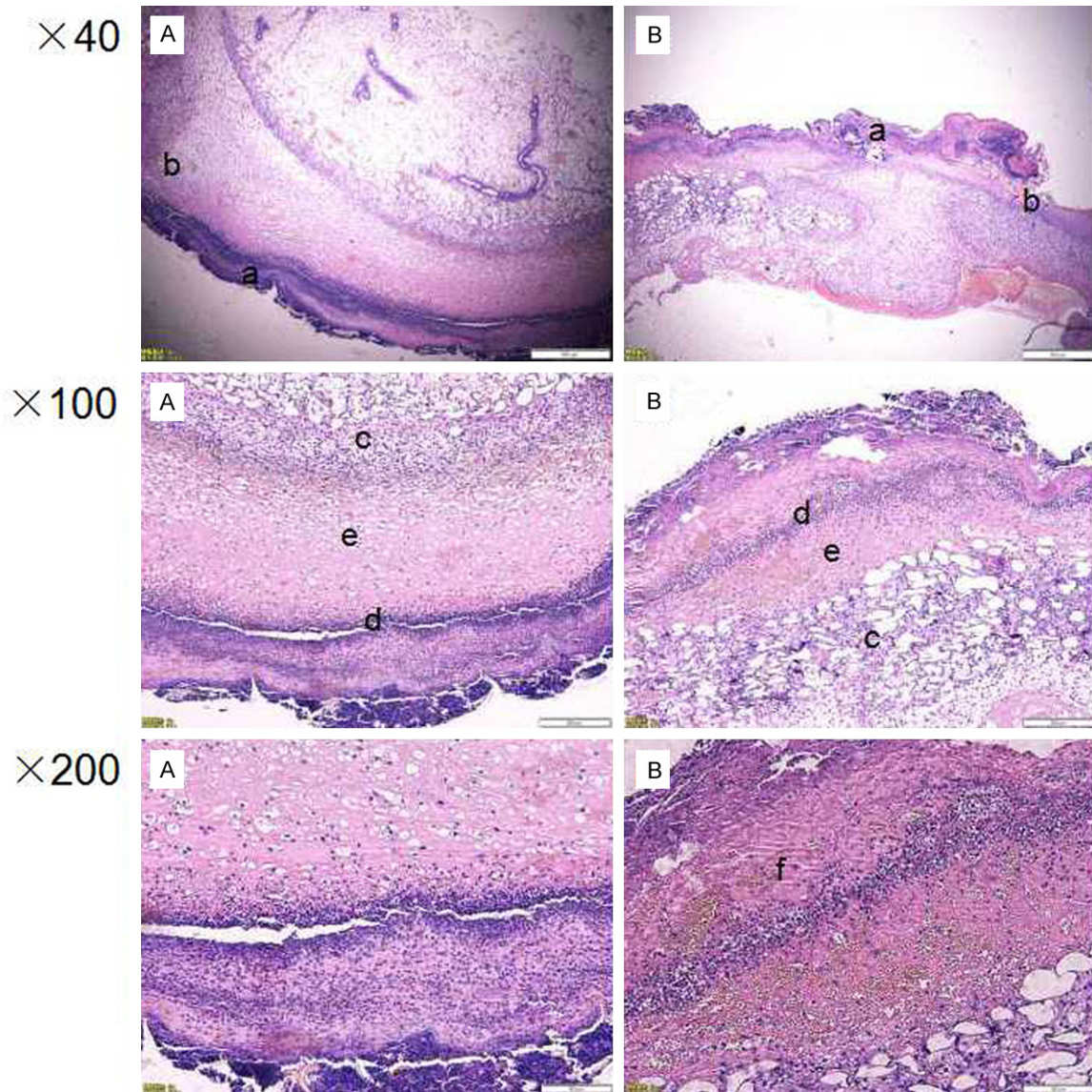
Figure 3. Representative micrographs of wound healing on day 3 (HE staining) in the control group (A) and treatment group (B) under ×40, ×100, and ×200 magnifications. Crusts (a), new skin tissue (b), new granulation tissue (c), tissue necrosis (d), exudates (e), and scaffold (f).

both groups, although that remaining in the control group was much thicker than that in the treatment group (**Figure 4**, ×40, ×100). The scaffold in the treatment group had completely dissolved and was invisible. In the treatment group, the granulation tissue base had a uniform thickness and an abundance of new capillaries with a distinct lumen full of erythrocytes had formed. In contrast, the thickness of granulation tissue was uneven in the control group and new capillaries, mostly presented a slit-like appearance, with the rare occurrence erythrocytes in the lumen (**Figure 4**, ×400).

On day 14, the wound surface in the control group was covered with thick crusts, which separated from the tissue after section, while detached crusts were evident in the treatment group. In both groups, the surface of the whole wound was covered with epidermal tissue but without exudate and necrosis, and keratinization was evident. Keratinized substances had accumulated and the thickness of the stratified squamous epithelium was uneven in the control group, while the epithelium thickness of the treatment group was uniform (**Figure 5**, ×40, ×100). As shown in **Figure 5**, there was no epi-
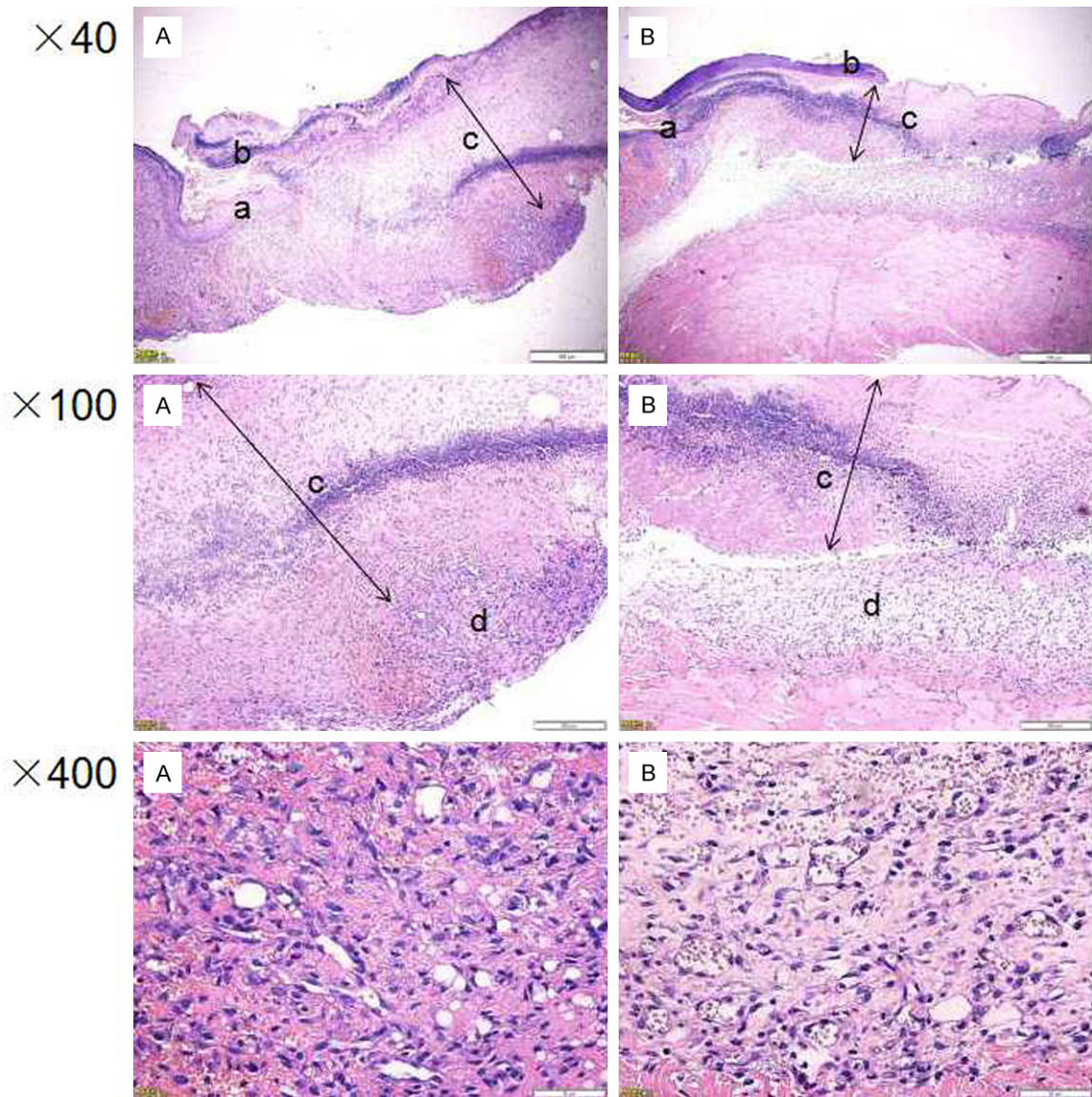
Figure 4. Representative micrographs of wound healing on day 7 (HE staining) in the control group (A) and treatment group (B) under ×40, ×100, and ×400 magnifications. New epidermis (a), crusts (b), exudates and necrosis (c + double arrow), and new granulation tissue (d).

thelial corner and dermal papilla in the stratified squamous epithelium of either group. Granulation tissues beneath all wounds had matured to form scar tissues but more, fresh granulation tissues were still visible in the deep layer of the control group (**Figure 5**, ×100). Edema was substantially relieved and abundant red-stained collagen fibers were observed in both groups. However, the control group, still had more capillaries with dilated lumen, more fibroblasts, and loose collagen fibers, while there were fewer fibroblasts, more mature fibrocytes, and dense collagen fibers in the treatment group (**Figure 5**, ×400).

Discussion

As a type of carrier for cell adhesion and proliferation, bioactive scaffolds may promote the formation of new tissues. They can also be a crucial factor in skin tissue engineering as a platform to guide cell restructuring and subsequent skin tissue regeneration [14-16]. At present, most animal experiment studies about skin tissue engineering in wound healing have focused on the rate of wound healing but ignored histopathological analysis in wound healing process [10, 17]. In this study, we not only observed changes in the surface of the
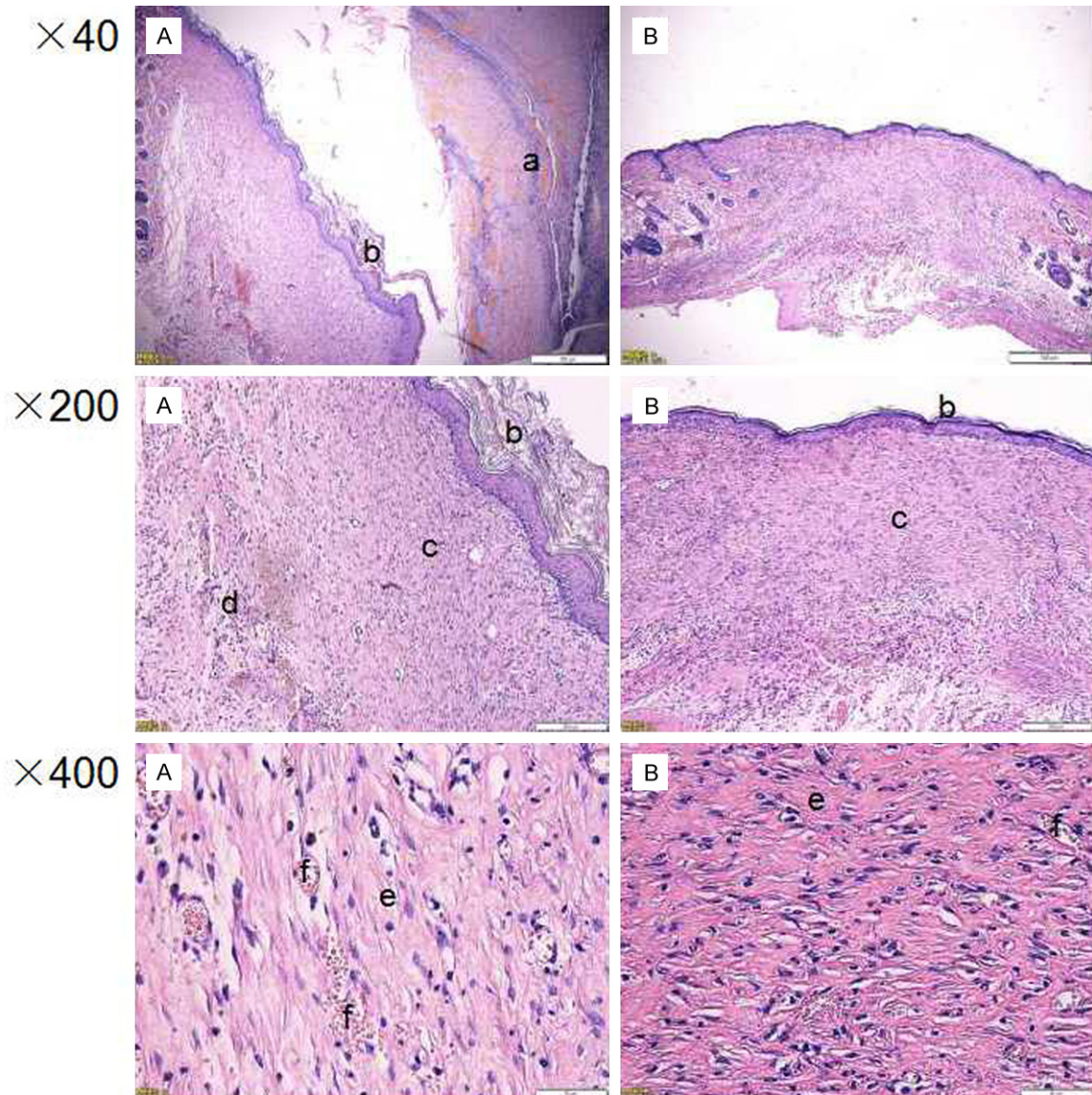
Figure 5. Representative micrographs of wound healing on day 14 (HE staining) in the control group (A) and treatment group (B) under ×40, ×100, and ×400 magnifications. Crusts (a), keratinized substances (b), scar tissue (c), granulation tissue (d), collagen fibers (e), and capillaries with dilated lumen (f).

animal wounds at various time points but also analyzed the histopathological morphology and healing process of various wounds.

This study showed that in comparison to the control group, the use of gelatin-alginate scaffolds can decrease wound bleeding and evident exudation at the early stage of the injury, while promoting the exudates of inflammatory cells, the formation of fibrocytes and dense collagen in the process of wound healing, which facilitated scar tissue maturation and accelerated healing process. Compared to the control

group, the treatment group realized faster wound recovery and closure (**Figure 2**).

With no cytotoxicity and immunogenicity, gelatin and alginate are ideal biological materials that benefit cell adhesion and absorption of wound exudates, thus, promote the inflammatory response and accelerate wound healing [18]. In this study, the use of gelatin-alginate scaffolds on the surface of mouse wounds absorbed the exudates and necrosis at the early stage of the wound healing process, which assisted thinner crust formation in the treat-

ment group than the control group (**Figure 3**, ×100 and **Figure 4**, ×100). Furthermore, compared to the control group, the treatment group formed more uniform and orderly granulation tissue (**Figure 4**, ×100 and **Figure 5**, ×400), which demonstrated that bioactive gelatin-alginate scaffolds provided a platform for cell migration and proliferation [19]. Moreover, the uniform and orderly porous structure of gelatin-alginate, divided large skin trauma into multiple tiny wounds, guided granulation tissue growth from the base of the wound, decreased the healing difficulty of large trauma, and formed orderly granulation tissue and mature capillaries (**Figure 5**, ×400). On this basis, a certain height of the granulation tissue in the treatment group created conditions for growth and migration of epidermal cells [20] to realize epidermal tissue cover on the wounds and form a stratified squamous epithelium of uniform thickness (**Figure 5**, ×40, ×100).

Wound healing is a complicated and continuous physiological process [21], involving an inflammatory response, cell proliferation, connective tissue formation, wound contraction, and reconstruction. Understanding the physiological process of wound healing is crucial to facilitate wound healing. Equally, understanding the process of pathological changes after applying gelatin-alginate scaffolds to mouse wounds is also vital. Tong *et al.* [10] implanted bone marrow mesenchymal stem cells (BMSCs) after hypoxic preconditioning into collagen-chitosan scaffolds that were applied to wound models in diabetic rats to study the attachment of BMSCs to the scaffolds and the promotion of the scaffolds to the rate of wound healing, inflammatory cell exudates, and angiogenesis. Wang *et al.* [17] primarily studied the scaffold properties *in vitro* and observed the wound healing rate after applying collagen/HA/gelatin scaffolds to mouse wounds but overlooked the histopathological analysis during mouse tissue reconstruction. Therefore, our research filled this blank.

As the most common method for histopathology, HE staining is mainly used to assess the fibroblast number, collagen content, and angiogenesis, epithelial formation during the skin healing process [22]. The present study, used HE staining and histopathological analysis, to identify the early stage of wound healing. The covering of wounds by gelatin-alginate scaffolds decreased hemorrhage and exudation on the wound surface to form a thin crust. At the middle stage of healing, the treatment group formed granulation tissue with uniform thickness and more mature new capillaries than the control group. At the later stage of healing, in the scaffold group, the crusts detached earlier than the control group, the accumulation of keratinized substances decreased, thus, squamous epithelium of uniform thickness and dense collagen fibers formed, which accelerated the rate of wound healing. Meanwhile, the strength and tension resistance of the wounds in the treatment group increased, enhancing the quality of wound healing. The systematic and detailed histopathological analysis of the wound healing process provided direct evidence to better understand the effects of gelatin-alginate, encouraging further research and use of gelatin-alginate scaffolds. In addition, the elaborate histopathological study provides more research direction ideas in animal experiments of tissue engineering.

In conclusion, the use of 3D bioprinting porous scaffolds on the surface of mouse wounds shortened the wound healing time (2 days). At the early and middle stage, the scaffolds decreased necrosis, hemorrhage and inflammatory exudation to form thinner crusts than the control group. At the middle stage, the scaffolds promoted the formation of granulation tissue with uniform thickness, the maturation of new capillaries, and decreased swelling. At the later stage, the scaffolds accelerated the detachment of the crusts, decreased the accumulation of keratinized substances, and facilitated the regeneration of squamous epithelium of uniform thickness and formation of dense collagen fibers, and thus, increased the strength and tension resistance of scar tissue.

Acknowledgements

Disclosure of conflict of interest

None.

Address correspondence to: Fang Gu, Qingdao University Medical College, 38 Dengzhou Road, Qingdao 266000, Shandong, China. Tel: +86-532-837800-61; Fax: +86-532-83780061; E-mail: gufang61@yeah.net; Dr. Jie Liu, The Affiliated Hospital of Qingdao University, 16 Jiangsu Road, Qingdao 266071, Shandong, China. E-mail: 18661801995@163.com

References

[1]   Langer R. Perspectives and challenges in tissue engineering and regenerative medicine. Adv Mater 2009; 21: 3235-3236.

[2]   Bullough L, Johnson S and Forder R. Evaluation of a foam dressing for acute and chronic wound exudate management. Br J Community Nurs 2015; Suppl Wound Care: S17-18, S20, S22-14.

[3]   Michael S, Sorg H, Peck CT, Koch L, Deiwick A, Chichkov B, Vogt PM and Reimers K. Tissue engineered skin substitutes created by laser-assisted bioprinting form skin-like structures in the dorsal skin fold chamber in mice. PLoS One 2013; 8: e57741.

[4]   Leong KF, Cheah CM and Chua CK. Solid free-form fabrication of three-dimensional scaffolds for engineering replacement tissues and organs. Biomaterials 2003; 24: 2363-2378.

[5]   Ehrenreich M and Ruszczak Z. Tissue-engineered temporary wound coverings. Important options for the clinician. Acta Dermatovenerol Alp Pannonica Adriat 2006; 15: 5-13.

[6]   Lee KY and Mooney DJ. Alginate: properties and biomedical applications. Prog Polym Sci 2012; 37: 106-126.

[7]   Ma L, Gao C, Mao Z, Zhou J, Shen J, Hu X and Han C. Collagen/chitosan porous scaffolds with improved biostability for skin tissue engineering. Biomaterials 2003; 24: 4833-4841.

[8]   Dean DM, Napolitano AP, Youssef J and Morgan JR. Rods, tori, and honeycombs: the directed self-assembly of microtissues with prescribed microscale geometries. FASEB J 2007; 21: 4005-4012.

[9]   Li DM, Krantz WB, Greenberg AR and Sani RL. Membrane formation via thermally induced phase separation (TIPS): model development and validation. J Memb Sci 2006; 279: 50-60.

[10]   Tong C, Hao H, Xia L, Liu J, Ti D, Dong L, Hou Q, Song H, Liu H, Zhao Y, Fu X and Han W. Hypoxia pretreatment of bone marrow-derived mesenchymal stem cells seeded in a collagen-chitosan sponge scaffold promotes skin wound healing in diabetic rats with hindlimb ischemia. Wound Repair Regen 2016; 24: 45-56.

[11]   Stachewicz U, Qiao T, Rawlinson SCF, Almeida FV, Li WQ, Cattell M and Barber AH. Microscopy and supporting data for osteoblast integration within an electrospun fibrous network. Data Brief 2015; 5: 775-781.

[12]   Shi HF, Han CM, Mao ZW, Ma L and Gao CY. Enhanced angiogenesis in porous collagen-chitosan scaffolds loaded with angiogenin. Tissue Eng Part A 2008; 14: 1775-1785.

[13]   Ansell DM, Holden KA and Hardman MJ. Animal models of wound repair: are they cutting it? Exp Dermatol 2012; 21: 581-585.

[14]   Karande TS, Ong JL and Agrawal CM. Diffusion in musculoskeletal tissue engineering scaffolds: design issues related to porosity, permeability, architecture, and nutrient mixing. Ann Biomed Eng 2004; 32: 1728-1743.

[15]   Hollister SJ. Porous scaffold design for tissue engineering. Nat Mater 2005; 4: 518-524.

[16]   Stevens MM and George JH. Exploring and engineering the cell surface interface. Science 2005; 310: 1135-1138.

[17]   Wang HM, Chou YT, Wen ZH, Wang ZR, Chen CH and Ho ML. Novel biodegradable porous scaffoldapplied to skin regeneration. PLoS One 2013; 8: e56330.

[18]   Freyman TM, Yannas IV and Gibson LJ. Cellular materials as porous scaffolds for tissue engineering. Proa Mater Sci 2001; 46: 273-282.

[19]   Pereira RF, Barrias CC, Granja PL and Bartolo PJ. Advanced biofabrication strategies for skin regeneration and repair. Nanomedicine 2013; 8: 603-621.

[20]   Trexler RA. Assessment of surgical wounds in the home health patient: definitions and accuracy with OASIS-C. Home Healthc Nurse 2011; 29: 550-559.

[21]   Velnar T, Bailey T and Smrkolj V. The wound healing process: an overview of the cellular and molecular mechanisms. J Int Med Res 2009; 37: 1528-1542.

[22]   Gonzalez VC, Beheregaray AC, Peres BM, Sallis ES, Varela Junior AS and Trindade GS. Histopathological analysis of UVB and IR interaction in rat skin. Photochem Photobiol 2015; 91: 895-900.